Universiteit Leiden
The Netherlands

Novel immune cell-based therapies for atherosclerosis

Frodermann, V.

Citation
Frodermann, V. (2015, May 27). *Novel immune cell-based therapies for atherosclerosis*. Retrieved from https://hdl.handle.net/1887/33064

Version:	Corrected Publisher's Version
License:	Licence agreement concerning inclusion of doctoral thesis in the Institutional Repository of the University of Leiden
Downloaded from:	https://hdl.handle.net/1887/33064

Note: To cite this publication please use the final published version (if applicable).

Cover Page

Universiteit Leiden

Leiden University Repository

The handle http://hdl.handle.net/1887/33064 holds various files of this Leiden University dissertation

Author: Frodermann, Vanessa
Title: Novel immune cell-based therapies for atherosclerosis
Issue Date: 2015-05-27

Vanessa Frodermann[1]
Gijs H.M. van Puijvelde[1]
Menno Hoekstra[1]
Gerjan de Bruin[2]
Janine van Duijn[1]
Thomas van der Heijden[1]
Mara J. Kröner[1]
Peter J. van Santbrink[1]
Herman S. Overkleeft[2]
Ilze Bot[1]
Bogdan I. Florea[2]
Saskia C.A. de Jager[1,3]
Johan Kuiper[1]

7

[1] Division of Biopharmaceutics, LACDR, Leiden University, Leiden, The Netherlands
2 Leiden Institute of Chemistry and Netherlands Proteomics Centre, Leiden, The Netherlands
[3] Present address: Laboratory of Experimental Cardiology, University Medical Center Utrecht, Utrecht, The Netherlands

Bortezomib: A Novel Lipid-Lowering Drug to Prevent Atherosclerosis

Manuscript in preparation.

Abstract

Objective The ubiquitin-proteasome system plays a key role in cellular protein homeostasis. It degrades the majority of proteins, e.g. cell cycle proteins, apoptotis-regulating proteins, and transcription factors. We assessed whether proteasome inhibition in addition to its effect on inflammation could affect lipid metabolism in atherosclerosis-prone low-density lipoprotein receptor-deficient ($LDLr^{-/-}$) mice.

Methods and Results We found that proteasome inhibition by Bortezomib treatment during eight weeks of Western-type diet resulted in a robust 59% reduction of aortic root lesion sizes in $LDLr^{-/-}$ mice. These lesions show a 1.9-fold reduction in macrophage numbers. Overall, proteasome inhibition significantly reduced inflammation and resulted in reduced aortic VCAM-1 expression, reduced plasma CCL2 levels, and reduced monocyte and macrophage responses. Moreover, pro-atherogenic Th1 responses were decreased and T cells were skewed towards Th2 responses.

Bortezomib also significantly reduced plasma cholesterol levels by 50% due to a significant 62% decrease in plasma very low-density lipoprotein (VLDL) levels. VLDL secretion rates were decreased by 50% in Bortezomib-treated mice, resulting from reduced *de novo* hepatic synthesis of lipids, as determined by a significant 58% reduction of fatty acid synthase. Moreover, increased cholesterol efflux to the bile was observed, as determined by a 2-fold upregulation of ABCG5.

Conclusion Our results show a previously unknown effect of proteasomal inhibition by Bortezomib on dyslipidemia, making proteasome inhibition a very potent target for cardiovascular diseases as dual reduction of inflammation and dyslipidemia can be achieved. Targeting the proteasome may thus be especially beneficial for the treatment of atherosclerosis in statin-unresponsive patients.

Introduction

The 26S proteasome is the primary enzyme complex responsible for protein degradation in mammalian cells[1]. Multiple proteins are targeted for proteasomal degradation by ubiquitination: cell cycle- and apoptosis-regulating proteins, damaged or misfolded proteins, and antigens for major histocompatibility complex (MHC) I presentation[1,2]. As such, the proteasome plays a central role in cellular homeostasis and controls cell cycle progression, differentiation, apoptosis, cellular stress responses and immune responses[3]. Dysregulation of the ubiquitin proteasome system is associated with multiple diseases, such as cancer, neurodegenerative diseases, viral infections, cardiovascular disease and autoimmune diseases[2,4,5].

The mammalian 26S proteasome consists of a barrel-shaped 20S core protein subunit and one or two regulatory cap proteins, which recognize polyubiquitinated proteins and move them to the 20S core[6]. The 20S core degrades proteins in its hollow center and consists of seven α and seven β subunits, of which β1, β2 and β5 have proteolytic activity. The β1 subunit has caspase-like activity, the β2 subunit has trypsin-like activity and the β5 subunit has chymotrypsin-like activity[7]. During inflammation or cellular stress these catalytic subunits are constitutively replaced by the inducible β subunits β1i (LMP2), β2i (MECL-1) and β5i (LMP7). This switch to the "immunoproteasome" is induced by IFN-γ and/or TNF-α and shows enhanced protein processing capacity, resulting in increased MHC I peptide presentation[8,9].

Proteasomal inhibition has been thoroughly investigated in cancer. Initial interest was driven by studies showing that proteasomal inhibitors could block anti-apoptotic nuclear factor (NF)-κB signaling, thereby inducing apoptosis in cancer cells. The inhibition of NF-κB signaling by proteasome inhibitors was attributed to the accumulation of IκBα, an inhibitor of NF-κB, and the lack of proteolytic processing of the p100 precursor of p52 needed for non-canonical NF-κB signaling[10]. However, recent studies suggest that proteasomal inhibition can also induce NF-κB signaling by upregulation of RIP2 and IKKβ, which decrease levels of inhibitory IκBα[11,12]. Besides this proposed effect on NF-κB signaling, proteasome inhibitors have been found to induce cell cycle arrest and degradation of pro-apoptotic factors, e.g. p53, NOXA and Bim[10], in cancer cells. Moreover, proteasome inhibitors result in reduced angiogenesis, by decreasing vascular endothelial growth factor (VEGF) and suppressing proliferation of vascular endothelial cells[13].

Due to its effect on NF-κB, proteasome inhibition has also been investigated in inflammation, as the NF-kB pathway is induced via ligation of Toll-like receptors, CD40, TNF receptors, IL-1 receptor, and the T cell receptor[14]. Indeed, treatment of macrophages with proteasome inhibitors reduced TLR-induced responses, such as iNOS, TNF-α, and IL-6 induction[15]. Proteasome inhibition has been shown to be protective in experimental models of (collagen-induced) arthritis[16,17], acute graft-versus-host disease[18,19], and experimental autoimmune encephalomyelitis[20].

The most well-known and best studied proteasome inhibitor is the reversible dipeptidyl boronic acid inhibitor Bortezomib (PS-341, Velcade®) which primarily blocks β5 and β5i subunits, but also β1 and β1i[3]. It has been approved by the

United States Food and Drug Administration (FDA) for the treatment of multiple myeloma and mantle cell lymphoma[21]. Proteasomal inhibition has been previously addressed in atherosclerosis. Herrmann *et al.* have found increased atherosclerosis in a pig model of diet-induced atherosclerosis due to increased oxidative stress[22]. In ApoE$^{-/-}$ mice no effect on early atherosclerotic lesions was found, but in advanced stages of atherosclerosis Bortezomib induced rupture-prone lesions, likely due to increased smooth muscle cell and macrophage apoptosis[23]. Wilck *et al.*, however, describe reduced atherosclerosis in LDLr$^{-/-}$ mice due to anti-inflammatory and anti-oxidative effects of Bortezomib[24].

Interestingly, mutations in the β5i gene have been shown to correlate with reduced adipose tissue in humans[25]. Recently, a study by Oliva *et al.* has found that Bortezomib reduces ethanol-induced steatosis by downregulation of several lipogenic genes[26]. We therefore hypothesized that Bortezomib, in its actual therapeutic dose, could not only reduce inflammatory responses but also beneficially affect dyslipidemia. Indeed, in this study we show that Bortezomib reduces atherosclerosis in LDLr$^{-/-}$ mice in part via a reduction in inflammation but also in part via a novel, previously unrecognized, effect of Bortezomib on lipid metabolism and VLDL secretion.

Material and Methods

Animals

C57BL/6 and LDLr$^{-/-}$ mice were originally obtained from the Jacksons Laboratory, kept under standard laboratory conditions, and administered food and water *ad libitum*. All animal work was approved by the Ethics Committee for Animal Experiments of Leiden University and conforms to Dutch government guidelines.

Atherosclerosis

Atherosclerosis was induced in 10-12 weeks old female LDLr$^{-/-}$ mice by feeding a Western-type diet (WTD; 0.25% cholesterol and 15% cocoa butter; Special Diet Services) for eight weeks. Mice were treated twice weekly *intraperitoneally* with 0.5 mg/kg Bortezomib or PBS containing DMSO as a vehicle control. Treatment was started one week prior to WTD and continued during the entire experiment. A 20mM stock solution of Bortezomib was made in DMSO und adjusted to the final concentration, which was on average 0.0125 mg/mouse, in PBS. All solutions were prepared prior to injections after determination of the weight of the mice.

Proteasomal Activity-Based Protein profiling

Proteasomal activity was determined as previously described[27]. Briefly, samples were treated with lysis buffer (50 mM Tris, pH 7.5, 10% glycerol, 5 mM $MgCl_2$, 2 mM ATP and 2 mM DTT, 20-50 µL) for 1 hour on ice, followed by centrifugation at 14 000 rpm for 10 min. Samples containing 10 µg/9 µL protein (protein concentration determined using Qubit® protein assay kit) were then incubated for 1 hour with BODIPY(FL)-epoxomicin (1 µL, 0.5 µM end concentration; developed at the Leiden Institute of Chemistry) at 37°C. Next, Laemmli sample buffer (4x, 4 µL) was added and samples

were boiled for 3 minutes. Gel electrophoresis was performed on a 12.5% SDS-PAGE (15 min 80 V, 120 min 120 V). In-gel detection of residual proteasome activity was performed in the wet gel slabs directly on a ChemiDoc MP system using Cy3 settings.

In vivo hepatic VLDL production rate

Mice were fasted for 16 hours prior to the experiment. At t=0 min, venous blood was drawn from the tail vein and mice were subsequently injected *intravenous* with 500 mg/kg Triton WR-1339 (Sigma-Aldrich) to inhibit lipoprotein lipase and prevent lipolysis of newly secreted hepatic VLDL. Additional tail vein blood samples were taken after 60, 120, and 180 min to determine VLDL-triglyceride (TG) levels. The VLDL-TG secretion rate was determined by the slope of the TG rise over time by linear regression analysis.

Tissue lipid analysis

Lipids were extracted from liver using the Folch method as described previously[28]. Briefly, 100 mg of tissue was homogenized with chloroform/methanol (1:2). The homogenate was centrifuged to recover the upper phase, which was further washed with chloroform–0.9% NaCl (1:1, pH 1.0). After centrifugation, the lower chloroform phase containing lipids was evaporated and the retained lipids were solubilized in 2% Triton X-100 by sonication. Protein content of the tissue homogenates was analyzed by BCA assay (Pierce Biotechnology, Thermo Fisher Scientific). Total cholesterol and triglyceride contents of the lipid extract were determined using enzymatic colorimetric assays (Roche Diagnostics). Data were expressed relative to the protein content.

Plasma cholesterol levels and FPLC seperation

Plasma concentrations of total cholesterol were determined by enzymatic colorimetric assays (Roche Diagnostics). Absorbance was read at 490 nm. Precipath (standardized serum; Roche Diagnostics) was used as internal standard. The distribution of cholesterol over the different lipoproteins in plasma was determined by fractionation of 30 µl of plasma of each mouse using a Superose 6 column (3.2 x 300 mm, Smart-System; Pharmacia). Total cholesterol content of the effluent was determined as described above.

$CD4^+$ T cell isolation and proliferation

Single cell suspensions of spleens from $LDLr^{-/-}$ mice were obtained by using a 70 µm cell strainer (VWR International). Red blood cells were lysed with erythrocyte lysis buffer (0.15 M NH_4Cl, 10 mM $NaHCO_3$, 0.1 mM EDTA, pH 7.3). $CD4^+$ T cells (>95% purity) were isolated from splenocytes by using the $CD4^+$ T cell isolation kit according to manufacturer's protocol (Miltenyi Biotec). 1 x 10^5 $CD4^+$ T cells were cultured in 96-well plates (Greiner Bio-One) in the presence or absence of αCD3 and αCD28 (1 µg/mL, eBioscience) for 72 hours in complete RPMI 1640, supplemented with 10% FCS, 100 U/ml penicillin/streptomycin, 2mM L-glutamine (all obtained from PAA) and 20 µm β-mercaptoethanol (Sigma Aldrich). Proliferation was measured by addition of ^3H-thymidine (0.5 µCi/well, Amersham Biosciences) for the last 16 hours of culture.

The amount of ^{3}H-thymidine incorporation was measured using a liquid scintillation analyzer (Tri-Carb 2900R) as the number of disintegrations per minute (dpm). T cell subsets were determined by flow cytometry.

Real-time PCR

mRNA was isolated from the aortic arch and liver using the guanidium isothiocyanate method and reverse transcribed (RevertAid Moloney murine leukemia virus reverse transcriptase). Quantitative gene expression analysis was performed on a 7500 Fast real-time PCR system (Applied Biosystems) using SYBR Green technology. The expression was determined relative to the average expression of three household genes: Succinate dehydrogenase complex, subunit A, flavoprotein (Sdha), hypoxanthine phosphoribosyltransferase (HPRT), and 60S ribosomal protein L27 (Rpl27). For used primer pairs refer to Table 1.

Gene	*Forward*	*Reverse*
36B4	CTGAGTACACCTTCCCACTTACTGA	CGACTCTTCCTTTGCTTCAGCTTT
ABCG5	TGGCCCTGCTCAGCATCT	ATTTTTAAAGGAATGGGCATCTCTT
ABCG8	CCGTCGTCAGATTTCCAATGA	GGCTTCCGACCCATGAATG
CD36	ATGGTAGAGATGGCCTTACTTGGG	AGATGTAGCCAGTGTATATGTAGGCTC
CD68	TGCCTGACAAGGGACACTTCGGG	GCGGGTGATGCAGAAGGCGATG
DGAT	GGTGCCCTGACAGAGCAGAT	CAGTAAGGCCACAGCTGCTG
FAS	GGCGGCACCTATGGCGAGG	CTCCAGCAGTGTGCGGTGGTC
HPRT	TACAGCCCCAAAATGGTTAAGG	AGTCAAGGGCATATCCAACAAC
GAPDH	ATCCTGCACCACCAACTGCTTA	CATCACGCCACAGCTTTCCAG
LPL	CCCCTAGACAACGTCCACCTC	TGGGGGCTTCTGCATACTCAAA
LRP1	CTTCTGGTGGCTGGCGTGGTG	CATCCGCTGGTGCTGGAAGCC
MCP-1	CTGAAGCCAGCTCTCTCTTCCTC	GGTGAATGAGTAGCAGCAGGTGA
MTTP	TCTCACAGTACCCGTTCTTGGT	GAGAGACATATCCCCTGCCTGT
RPL27	CGCCAAGCGATCCAAGATCAAGTCC	AGCTGGGTCCCTGAACACATCCTTG
PPARγ	GACGCGGGCTGAGAAGTC	CACCGCTTCTTTCAAATCTTGTC
Scd1	TACTACAAGCCCGGCCTCC	CAGCAGTACCAGGGCACCA
SREBP-1C	TCTGAGGAGGAGGGCAGGTTCCA	GGAAGGCAGGGGGCAGATAGCA
VCAM-1	AGACTGAAGTTGGCTCACAATTAAGAAG	AGTAGAGTGCAAGGAGTTCGGG

Table 1. Primer Pairs used for qPCR analysis. The relative expression of genes was determined relative to the average expression of four housekeeping genes: ribosomal protein 36B4, glyceraldehyde 3-phosphate dehydrogenase (GAPDH), hypoxanthine-guanine phosphoribosyltransferase (HPRT), and ribosomal protein L27 (Rpl27). Abbreviations: ABCG5/8, ATP-binding cassette sub-family G member 5/8; DGAT, diglyceride acyltransferase; FAS, fatty acid synthase; LPL, lipoprotein lipase; LRP1, Low density lipoprotein receptor-related protein 1; MTTP, microsomal triglyceride transfer protein; PPARγ, peroxisome proliferator-activated receptor γ; Scd1; stearoyl-CoA desaturase-1; SREBP-1c, sterol regulatory element-binding protein 1; VCAM-1, Vascular cell adhesion protein 1.

Flow Cytometry

At sacrifice retro-orbital blood was collected and erythrocytes were lysed as described. Per sample, 3 x 10^5 white blood cells or 1 x 10^5 $CD4^+$ T cells from proliferation assays were stained with the appropriate antibodies. The following antibodies were used: CD11b-eFluor450 (clone M1/70), CD4-PerCP (clone RM4-5; BD Biosciences), CD25-FITC (clone eBio3C7), FoxP3-APC (clone FJK-16s), Gata-3-PE (clone TWAJ), Ly-6C-PerCP (clone HK1.4), Ly-6G-FITC (clone 1A8; BD Biosciences), RORγt-PE (clone AFKJS-9), and T-bet-APC (clone eBio4B10). All antibodies were purchased from eBioscience, unless stated otherwise. For intracellular staining, cells were fixed and permeabilized according to the manufacturer's protocol (eBioscience). Flow cytometry analysis was performed on the FACSCantoII and data were analyzed using FACSDiva software (BD Biosciences).

Cytokine and analysis

IL-2 and CCL2 were determined by ELISA, according to manufacturer's protocol (BD Biosciences).

Histological analysis

10 μm cryosections of the liver were stained with Oil-Red-O and hematoxylin to determine lipid content. To determine aortic root plaque size, 10 μm cryosections were stained with Oil-Red-O and haematoxylin (Sigma Aldrich). Corresponding sections were stained for collagen fibers using Sirius Red (Sigma Aldrich) and analyzed under polarized light. Macrophage content was analyzed by immunohistochemical staining against a macrophage-specific antigen (MOMA-2, polyclonal rat IgG2b, 1:1000, Serotec Ltd), respectively. Goat anti-rat IgG alkaline phosphatase conjugate (dilution 1:100; Sigma Aldrich) was used as a secondary antibody and nitro blue tetrazolium and 5-bromo-4-chloro-3-indolyl phosphate as enzyme substrates. To determine the number of adventitial T cells, CD3 staining was performed using anti-mouse CD3 (clone SP7, 1:150, ThermoScientific). BrightVision anti-rabbit-HRP was used as secondary antibody (Immunologic). The section with the largest lesion and four flanking sections were analyzed for lesion size and collagen content, two flanking sections were analyzed for macrophage and T cell content. All images were analyzed using the Leica DM-RE microscope and LeicaQwin software (Leica Imaging Systems). The percentage of collagen and macrophages in the lesions was determined by dividing the collagen- or MOMA-2-positive area by the total lesion surface area.

Statistical analysis

Values are expressed as mean±SEM. Data of two normally distributed groups were analyzed by Student's T-test, data of three groups were analyzed by one-way ANOVA and data of two or more groups with more than one variable were analyzed by two-way ANOVA, followed by Bonferroni post-testing. Statistical analysis was performed using Prism (GraphPad). Probability values of $P<0.05$ were considered significant.

Results

Bortezomib Reduces Proteasomal Activity in LDLr$^{-/-}$ Mice

Bortezomib is approved by the FDA for treatment of multiple myeloma and mantle cell lymphoma[21]. The recommended *intravenous* dose of Bortezomib in humans is 1.3 mg/m^2 (administered in cycles of twice weekly for 2 weeks followed by a 10-day rest period)[29]. Since this equals an *intravenous* dose of Bortezomib of about 0.42 mg/kg in mice[30], we chose to treat mice with an *intraperitoneal* dose of 0.5 mg/kg twice weekly, which is below the maximum tolerated dose in mice of 1.0 mg/kg twice weekly and this dose does not induce liver or kidney toxicity[17].

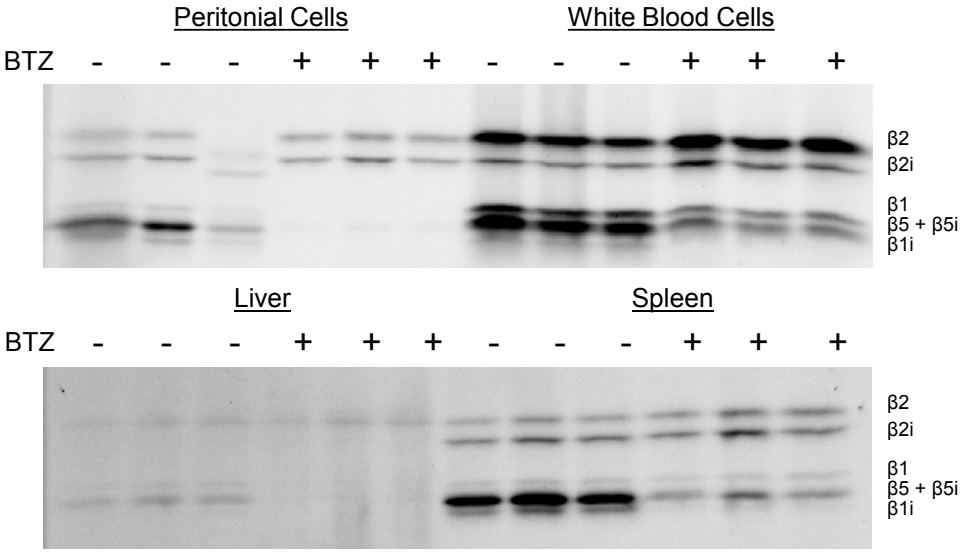

% inhibition	Peritoneal	Blood	Spleen	Liver
β1c	100	63	30	n.d.
β1i	100	n.d.	79	n.d.
β5	100	46	79	85

Figure 1. Bortezomib reduces proteasomal activity. Female LDLr$^{-/-}$ mice received two weekly injections of vehicle control (PBS/DMSO) or bortezomib (BTZ). One hour after the last injection, peritoneal cells, blood, liver cells, and splenocytes were isolated. Proteasome activity was determined by proteasomal activity-based profiling. Samples of three control mice and three mice treated with Bortezomib are shown. Table indicates average inhibition over three mice. Bands have been quantified and corrected for gel loading using coomassie quantification. n.d.: band could not be quantified due to overlap or too low intensity in samples.

To determine the extent of proteasome inhibition, we injected LDLr$^{-/-}$ mice with two weekly injections of Bortezomib after which we determined proteasome activity in peritoneal cells, white blood cells, liver and spleen. Peritoneal cell showed a complete inhibition of proteasome activity by the subunits β1, β1i, and β5/β5i. White blood cells in the circulation showed a 63% reduction of β1 and a 46% reduction of β5/β5i

subunits. Splenocytes showed a strong 79% inhibition of β1i and β5/β5i, while β1 was only inhibited by 30%. In the liver we found an 85% inhibition of β5/β5i subunits. No inhibition of β2 or β2i was observed. β5 and β5i subunits cannot be separated in murine samples by this analysis and their activity is therefore expressed together (Figure 1).

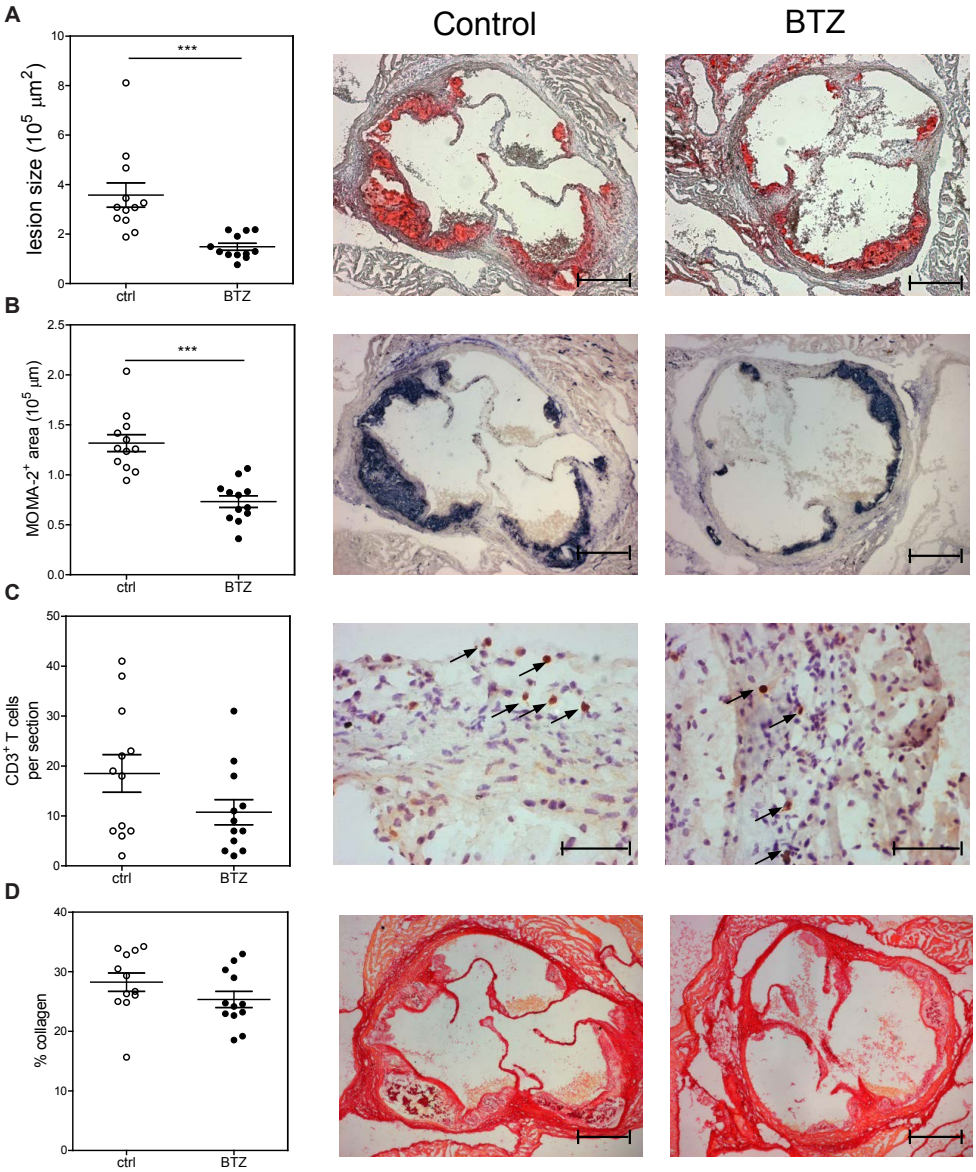

Figure 2. Bortezomib reduces atherosclerotic lesion development. A. At sacrifice, lesion size in the three valve area of the aortic root was determined; representative cross-sections stained with Oil-Red-O and hematoxylin are shown. Scale bar, 300 µm. **B.** Macrophage positive area was determined by MOMA-2 staining. Scale bar, 300 µm. **C.** CD3$^+$ T cells were determined by αCD3 staining. Arrows indicate T cells. Scale bar, 200 µm. **D.** Collagen positive area was determined by Sirius Red staining. Scale bar, 300 µm. All values are expressed as mean±SEM and are representative of six mice. *** P<0.001.

Proteasomal Inhibition Reduces Atherosclerotic Lesion Development

To assess the effect of proteasome inhibition on atherosclerosis, we treated female LDLr$^{-/-}$ mice twice weekly with *intraperitoneal* injections of Bortezomib. After one week, mice were put on a Western-type diet (WTD) for eight weeks to induce atherosclerotic lesion development. Bortezomib treatment was continued throughout the experiment. We observed a significant 58.6% reduction in lesion development (control: 3.6 x 10^5 ± 0.5 x 10^5 µm versus Bortezomib: 1.5 x 10^5 ± 0.1 x 10^5 µm; Figure 2A) and a 44.4% reduction in lesional macrophages (control: 1.3 x 10^5 ± 0.1 x 10^5 µm versus Bortezomib: 0.7 x 10^5 ± 0.1 x 10^5 µm; Figure 2B). The number of recruited CD3$^+$ T cells did not significantly differ (control: 18.5 ± 3.8 T cells per lesion versus Bortezomib: 10.7 ± 2.5 T cells per lesion; Figure 2C) and also no differences in collagen content of the lesions, as determined by Sirius red, were observed (control: 28.3 ± 1.5% versus Bortezomib: 25.3 ± 1.4%; Figure 2D).

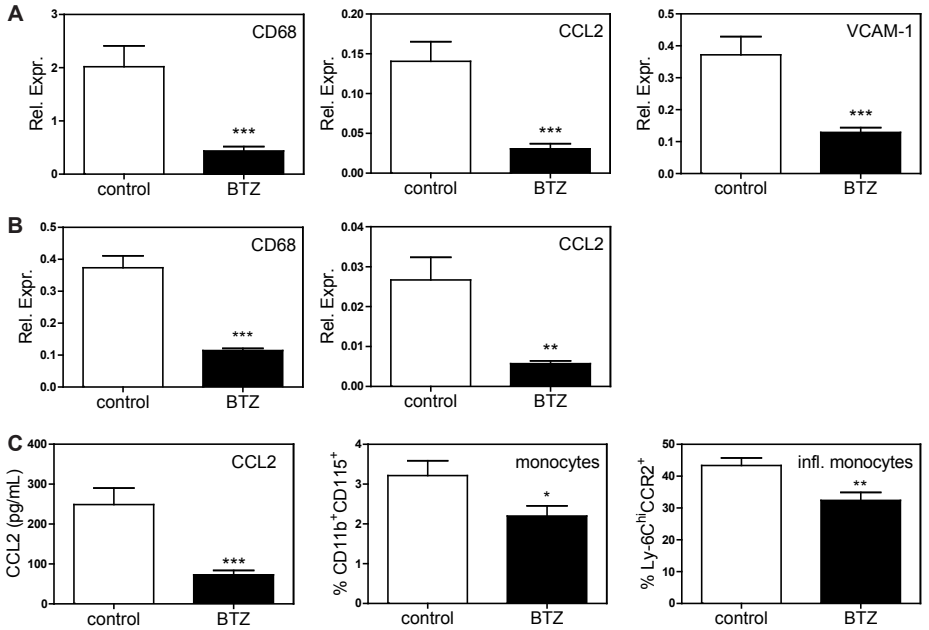

Figure 3. Bortezomib reduces monocytes and macrophages. A. The expression of CD68, CCL2 and VCAM-1 were determined in the aortic arch by qPCR. **B.** The expression of CD68 and CCL2 were determined in the liver by qPCR. Expression was determined relative to four housekeeping genes (36B4, GAPDH, HPRT, Rpl27). **C.** Serum CCL2 levels were determined by ELISA. Circulating monocytes and inflammatory monocytes as a percentage of total monocytes were determined by flow cytometry. All values are expressed as mean±SEM and are representative of at least six mice.* P<0.05, ** P<0.01, *** P<0.001.

Proteasomal Inhibition Significantly Reduces Monocyte Recruitment and Macrophages

In line with a reduction in lesional macrophages in the aortic root, we also observed a significant 78.4% reduced CD68 expression in the aortic arch of Bortezomib-treated mice indicative of reduced macrophages. This likely resulted from a reduced

recruitment of monocytes into the lesions as we observed a 77.9% reduced CCL2 and a 65.3% reduced VCAM-1 expression (Figure 3A). In the liver of Bortezomib-treated mice we also found a 69.4% reduction of CD68 expression and a 77.8% reduction of CCL2 expression (Figure 3B). Overall we established a 70.7% decrease in plasma CCL2 in the Bortezomib group: This corresponded with a 31.6% reduction in circulating monocytes and a 25.3% reduction in inflammatory Ly-6C^{hi}CCR2^{+} monocytes (Figure 3C).

Proteasomal Inhibition Skews T cells towards Th2 Responses and Reduces Th1 Responses

We argued that Bortezomib-treatment should affect T cell subset induction as proteasome inhibition has been suggested to preferentially induce Tregs and reduce Th1 and Th17 responses[31], although we did not observe significant effects on CD3^{+} T cells in the aortic root. We isolated splenic CD4^{+} T cells from Bortezomib-treated mice and control mice and induced general T cell proliferation by stimulation with αCD3 and αCD28 for 72 hours. We found a significant 43.4% and 72.8% reduced proliferative capacity, as determined by ^{3}H-thymidine incorporation and IL-2 production, respectively (Figure 4A). The relative percentages of T cell responses were significantly skewed towards Th2 responses, which were increased by 43.1%, while Th1 responses were decreased by 21.3% upon Bortezomib-treatment. Th17 responses were not affected and Treg percentages were slightly but non-significantly increased (Figure 4B), indicating that overall pro-atherogenic T cell responses were reduced after Bortezomib-treatment.

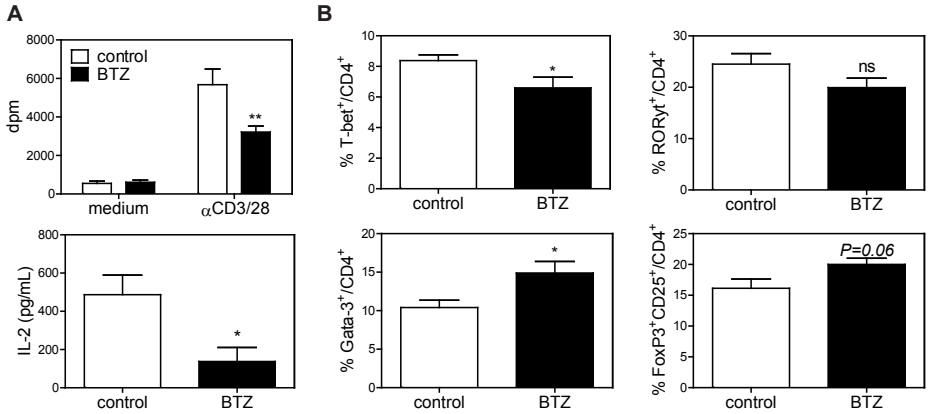

Figure 4. Bortezomib reduces T cell responses. A. Splenocytes were cultured in the presence of 1 µg/mL αCD3/αCD28 for 72 hours. Proliferation was assessed by the amount of ^{3}H-thymidine incorporation during the last 16 hours of culture and by IL-2 production determined by ELISA. **B.** Th1 (T-bet^{+}), Th2 (Gata-3^{+}), Th17 (RORγt^{+}) cells and Treg (FoxP3^{+}CD25^{+}) within CD4^{+} T cells were determined by flow cytometry. All values are expressed as mean±SEM and are representative of six mice.* P<0.05, ** P<0.01.

Proteasomal Inhibition Significantly Reduces Plasma Cholesterol and VLDL Secretion

During the entire experiment we monitored weight, food intake, plasma glucose and cholesterol levels to determine possible effects on metabolism. While we found no significant effects on food intake, weight development and plasma glucose levels (Figure 5A), we intriguingly observed that after one week WTD cholesterol levels plateaued in mice treated with Bortezomib. After eight weeks diet, proteasome inhibition resulted in a significant 50.2% decrease in total plasma cholesterol levels compared to control mice (Figure 5B). The large reduction in cholesterol levels was due to a substantial 62% decrease in plasma VLDL levels as determined by fast-performance liquid chromatography (FPLC) separation, while LDL and HDL levels were not affected (Figure 5B).

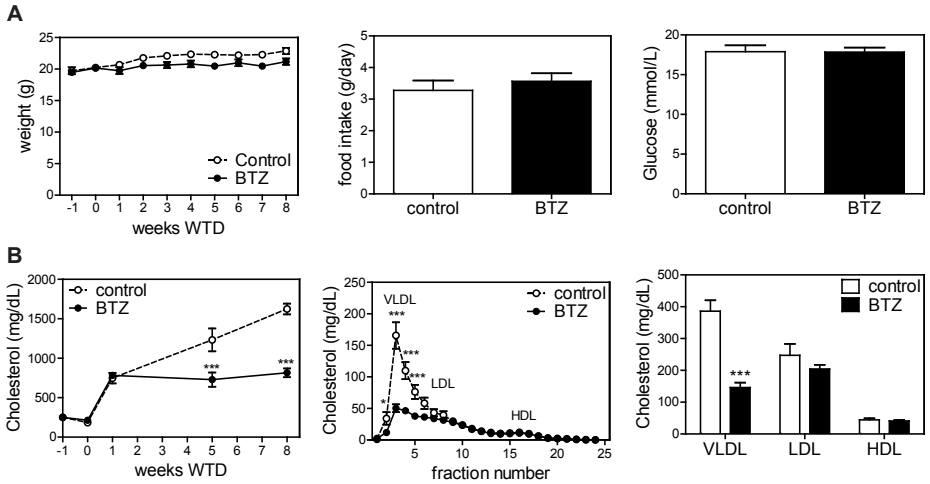

Figure 5. Bortezomib treatment reduces serum cholesterol levels. A. Mice were weighed weekly, food intake was determined during the last two weeks, and glucose was measured at the end of the experiment. **B.** Cholesterol levels were monitored throughout the entire experiment. For FPLC analysis 3 mice per group were pooled. Fractions 2–5 represent VLDL, fractions 6–14 represent LDL, and fractions 15–20 represent HDL. All values are expressed as mean±SEM and are representative of at least eight mice. * P<0.05, *** P<0.001.

Additionally, we observed a reduction in Oil-Red O positive staining in livers of Bortezomib-treated mice (Figure 6A). Oil-red O stains neutral lipids (e.g. triglycerides and cholesterol esters) and it is the most accurate method for determining the level of hepatic steatosis[32]. Steatosis, an abnormal lipid accumulation within cells, has been shown to be associated with an increased risk for atherosclerosis[33]. This finding indicates that Bortezomib-treated mice had significantly reduced WTD-induced liver steatosis and thereby decreasing a risk factor for atherosclerosis. Direct measurement of the cholesterol levels in the liver confirmed that cholesterol levels were decreased by 1.4-fold upon Bortezomib-treatment, while triglyceride content was not affected (Figure 6B).

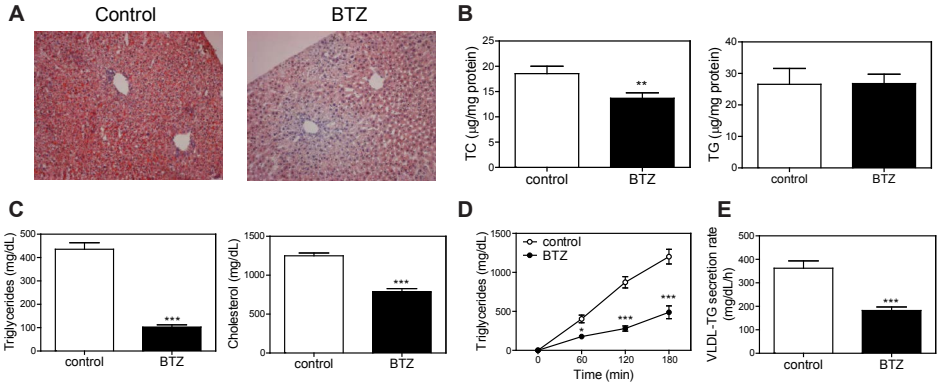

Figure 6. Bortezomib reduces VLDL secretion. A. Liver sections were stained with Oil-Red O, representative sections are shown. **B.** Cholesterol and triglyceride amounts per mg protein in the liver were determined. **C.** Female LDLr$^{-/-}$ were fasted for 16 hours after two weeks of WTD. Plasma Triglycerides and cholesterol levels were determined. **D.** Increases in triglyceride levels in circulation after administration of Triton WR-1339. **E.** VLDL-Triglyceride (TG) secretion determined over 180 min. All values are expressed as mean±SEM and are representative of six mice. * P<0.05, ** P<0.01, *** P<0.001.

To establish whether the reduction in plasma VLDL was associated with a reduction in VLDL secretion, we performed a Triton WR-1339 study. After two weeks WTD, when plasma cholesterol levels had plateaued in Bortezomib-treated mice, we fasted mice for 16 hours and found a significant 76% and 37% reduction in plasma triglycerides and cholesterol, respectively (Figure 6C). Subsequently, we injected Triton WR-1339 and found a significant reduction in the secretion of VLDL-triglycerides in Bortezomib-treated mice, when corrected for initial differences (Figure 6D). Overall, Bortezomib-treated mice showed a 49.6% reduction in their VLDL-triglyceride secretion rate (Figure 6E). Reduced VLDL secretion has often been seen to increase triglyceride content of the liver, but we did not observe any effect on liver triglyceride content.

Proteasomal Inhibition Significantly Reduces Lipogenesis and Increases Bile Acid Excretion

To determine if reduced VLDL secretion was due to reduced hepatic lipid uptake we assessed the expression of CD36 and LDL receptor-related protein 1 (LRP1), both receptors for VLDL and chylomicrons. CD36 and LRP1 were not affected by Bortezomib-treatment (Figure 7A), indicating that hepatic VLDL clearance from the circulation was not affected.

We further assessed whether expression of genes involved in hepatic *de novo* lipogenesis was modified. Fatty acid synthase (FAS) is the main biosynthetic enzyme in lipogenesis, which synthesizes palmitate from acetyl-CoA and malonyl-CoA. Interestingly, we observed a striking downregulation by 57.8%. Stearoyl-CoA desaturase-1 (Scd1) is the rate-limiting enzyme in the synthesis of unsaturated fatty acids further downstream of FAS, resulting in production of oleic acid. We found that Scd1 was also reduced by 44%, but this was not significant (Figure 7 B). In contrast, diglyceride acyltransferase 1 (DGAT1), which is involved in the last steps of triglyceride synthesis, and microsomal triglyceride transfer protein (MTTP), which plays a central

role in lipoprotein assembly, were not affected (Figure 7C).

Sterol regulatory element binding protein-1c (SREBP-1c), a transcription factor regulation *de novo* lipogenesis genes, was also not affected (Figure 7D). However, peroxisome proliferator-activated receptor γ (PPARγ), a transcription factor known to be involved in high fat diet-induced liver steatosis[34], was significantly downregulated by 28.6% in line with the observed reduction in steatosis (Figure 7D). Additionally, we found a significant increase of ABCG5 by 101.3% indicating increased efflux of cholesterol to the bile for excretion. However, ABCG8, which has the same role in the liver, was not affected (Figure 7E). Interestingly, expression of lipoprotein lipase (LPL), which hydrolyzes triglycerides from VLDL and chylomicrons into free fatty acids, was significantly decreased by 70.5% (Figure 7F). LPL is not expressed in adult liver but mainly expressed by macrophages[35]. Therefore reduced LPL levels likely simply reflect reduced hepatic macrophage content.

Overall Bortezomib-treated mice show profound effects on hepatic liver metabolism: cholesterol efflux to the bile is likely increased and *de novo* lipogenesis is significantly reduced, which ultimately results in reduced VLDL secretion.

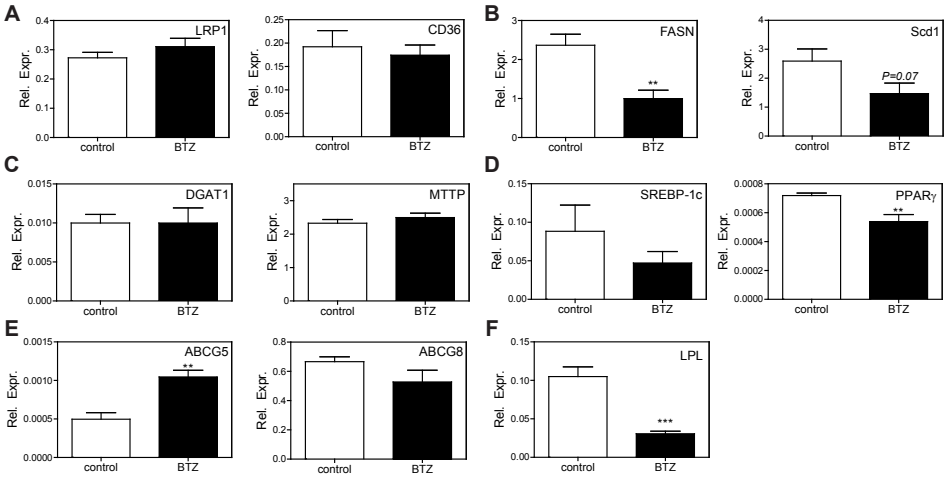

Figure 7. Bortezomib inhibits *de novo* lipogenesis. Genes involved in lipoprotein uptake (**A**), genes of key enzymes involved in initial steps of lipogenesis (**B**) and other further downstream enzymes of lipogenesis (**C**) , transcription factors (**D**), genes involved in cholesterol efflux (**E**) and lipoprotein lipase (**F**) were determined by qPCR. The expression is expressed relative to four housekeeping genes (36B4, GAPDH, HPRT, Rpl27). All values are expressed as mean±SEM and are representative of six mice. ** P<0.01, *** P<0.001.

Discussion

To our knowledge we show here for the first time that Bortezomib can have a potent lipid-lowering effect, a quality that in addition to its anti-inflammatory effects strengthens the beneficial effect of Bortezomib on atherosclerosis. Bortezomib is therefore the perfect dual drug to inhibit both underlying causes of atherosclerosis: inflammation and dyslipidemia. We find that as a result Bortezomib significantly

reduces atherosclerosis development by 58.6%.

We see a strong reduction of inflammatory responses. In line with an earlier atherosclerosis study by Wilck *et al.* we observe a significant reduction in VCAM-1, CCL2 levels and monocyte responses[24]. Moreover, we observe reduced Th1 cell induction and a skewing towards Th2 cells, which is in line with earlier described effects of proteasome inhibition on $CD4^+$ T cell subsets[31]. Anti-inflammatory effects of Bortezomib have also been described in experimental models for rheumatoid arthritis and graft-versus-host disease[17,18]. Interestingly, we see a large reduction of macrophage content in the liver. Uptake of oxLDL or cholesterol crystals has been found to increase expression of inflammatory genes in macrophages and may contribute to the development of hepatosteatosis[36,37]. Non-alcoholic steatohepatitis (NASH) is dramatically reduced when inflammatory responses of liver macrophages (Kupffer cells) are inhibited or reduced[36,38]. Therefore, an inhibition of pro-inflammatory responses in macrophages by Bortezomib could contribute to reduced steatosis.

In addition to reduced inflammation, we observed a robust decrease in plasma cholesterol and triglyceride levels, which was mainly the result of a robust reduction in circulating VLDL levels. We further determined that this reduction in VLDL was most likely related to multiple effects of Bortezomib. Bortezomib resulted in reduced *de novo* lipid synthesis due to a significant reduction of FAS expression and reduced hepatic cholesterol levels, which likely result from increased expression of liver ABCG5 and thus increased bile acid excretion (Figure 8). We additionally observed a very strong decrease of LPL. As LPL in the liver is mainly expressed by macrophages[35], it likely reflects decreases we observe in macrophage inflammation and numbers. However, LPL has been shown to promote foam cell formation[39] and reduced LPL expression in macrophages could thus contribute to the reduced cholesterol levels observed in the liver. Because LPL is secreted by macrophages, reduced hydrolysis of triglycerides from VLDL could result in less free fatty acid availability for VLDL production.

Information on the role of the ubiquitin-proteasome pathway in lipid metabolism is limited. A mutation in the PSMB8 gene, encoding β5i, results in reduced expression and reduced proteasome activity. This was found to induce loss of adipose tissue in the upper part of the human body by blocking adipocyte differentiation[25]. Interestingly, it was found that corticosteroid therapy reduces inflammation in these patients, but does not affect lipodystrophy, suggesting that effects on adipose tissue are likely not due to secondary effects of inflammation[25]. In the earlier atherosclerosis study by Wilck *et al.* changes in HMG-CoA reductase and HMG-CoA synthase in the aorta were observed[24], but they did not report on the expression of these genes in the liver. In a study by Oliva *et al.* Bortezomib was investigated in rats to determine possible beneficial effects on ethanol-induced steatosis. A reduction in several lipogenic genes, including SREBP-1c, FAS, Scd1, DGAT, HMG-CoA synthase, was observed, however, LPL in this study was significantly increased[26]. It has to be noted that in this study rats were on a normal chow diet. Interestingly, statins have been proposed to, besides their well-known effect on HMG-CoA reductase inhibition, also inhibit the proteasome[40,41]. However, whether this has any contribution to cholesterol-lowering capacities of statin treatment is unknown. Proteasome activator 28-null mice, which

show a 30-40% reduction of overall proteasomal activity, have increased SREBP-1c activity, hepatic steatosis and hepatic insulin resistance[42], indicating that the β2 and β2i subunits might have a beneficial effects on lipid metabolism as those are the only subunits not inhibited by Bortezomib. It will be interesting to determine if specific effects on one proteasomal subunit or combined inhibition are needed for the beneficial effect that Bortezomib exerts.

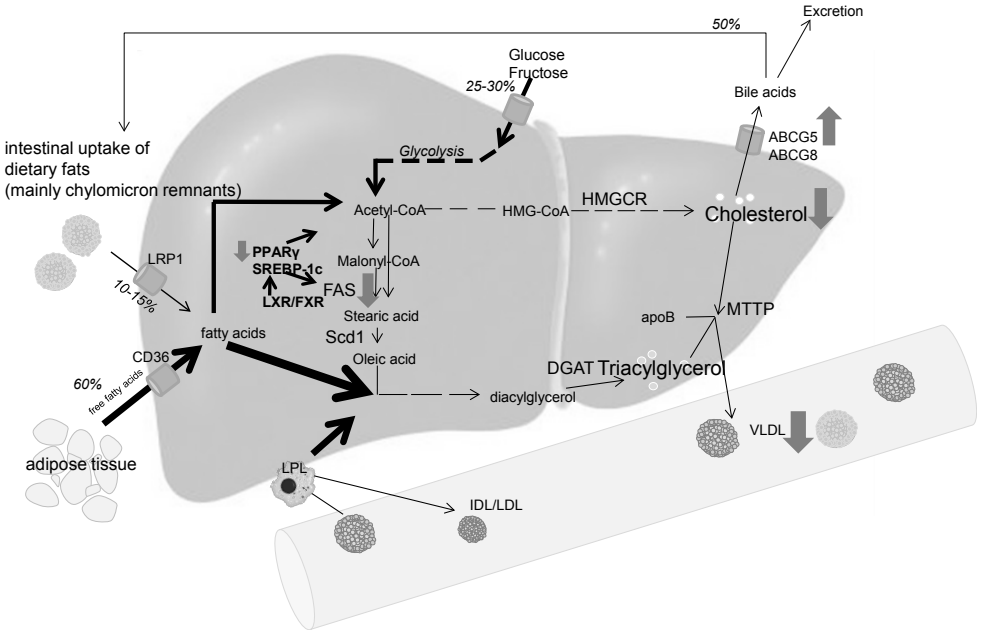

Figure 8. Scheme of Bortezomib effects on hepatic lipid metabolism. Bortezomib treatment did not affect lipoprotein uptake. However *de novo* lipogenesis is reduced, as FAS is significantly reduced, as well as PPARγ. Additionally ABCG5 is significantly increased resulting in increased cholesterol efflux. Overall this reduces hepatic cholesterol levels and reduced VLDL assembly, resulting in a decreased VLDL secretion rate. Grey arrows indicate positive effects of Bortezomib-treatment. Percentages indicate contribution to VLDL-triglycerides under conditions of non-alcoholic steatosis. ABCG5/8, ATP-binding cassette sub-family G member 5/8; DGAT, diglyceride acyltransferase; FAS, fatty acid synthase; HMGCR, 3-hydroxy-3-methyl-glutaryl-CoA reductase; LRP1, LDL receptor-related protein 1; PPARγ, peroxisome proliferator-activated receptor ; Scd1, Stearoyl-CoA desaturase-1; SREBP-1c, Sterol regulatory element binding protein-1c.

Bortezomib is already used in the clinic for multiple myeloma and it would be very interesting to determine whether patients receiving treatment show initial decreases in their plasma cholesterol levels after treatment. However, the cholesterol lowering effect of Bortezomib might have been overlooked as multiple myeloma patients have low basal cholesterol levels likely due to increased cholesterol utilization by myeloma cells[43]. After Bortezomib therapy patients did not show significant changes in their plasma cholesterol compared to pre-treatment values[43], indicating that a lower cholesterol level was maintained despite cancer remission.

The dramatic effect of Bortezomib-treatment on dyslipidemia is especially important as a substantial proportion of patients will not respond to statin treatment, either due to statin resistance or intolerance. Of patients receiving statin therapy only

73% will actually achieve target plasma LDL levels[44] and a large number of these patients will still have cardiovascular events[45]. Alternatives for patients unresponsive to statins include ezetimibe and bile acid sequestrants, but these treatments lack potency when compared to statin therapy[46]. For example, the use of ezetimibe in addition to statins was recently assessed in the IMPROVE-IT trial and found to reduce primary endpoint events, such as myocardial infarction and stroke, by only an additional 6.4%[47]. Nonetheless, a proportion of patients remain where none of the above mentioned therapies help to reduce plasma cholesterol, leaving these patients at a high risk for future cardiovascular complications. Currently, clinical trials establishing the effect of PCSK9 inhibition are ongoing and seem promising to reduce LDL levels. We show here that Bortezomib could be another potent alternative treatment, especially as it additionally significantly reduces inflammation. We envision that Bortezomib therefore will be a potent drug for the treatment of cardiovascular diseases due to its dual effects on inflammation and dyslipidemia.

References

1. Rock, K. L. *et al.* Inhibitors of the proteasome block the degradation of most cell proteins and the generation of peptides presented on MHC class I molecules. *Cell* 78, 761–71 (1994).
2. Wang, J. & Maldonado, M. A. The ubiquitin-proteasome system and its role in inflammatory and autoimmune diseases. *Cell. Mol. Immunol.* 3, 255–61 (2006).
3. Paniagua Soriano, G., De Bruin, G., Overkleeft, H. S. & Florea, B. I. Toward understanding induction of oxidative stress and apoptosis by proteasome inhibitors. *Antioxid. Redox Signal.* 21, 2419–43 (2014).
4. Pagan, J., Seto, T., Pagano, M. & Cittadini, A. Role of the ubiquitin proteasome system in the heart. *Circ. Res.* 112, 1046–58 (2013).
5. Ciechanover, A. & Brundin, P. The ubiquitin proteasome system in neurodegenerative diseases: sometimes the chicken, sometimes the egg. *Neuron* 40, 427–46 (2003).
6. Bedford, L., Paine, S., Sheppard, P. W., Mayer, R. J. & Roelofs, J. Assembly, structure, and function of the 26S proteasome. *Trends Cell Biol.* 20, 391–401 (2010).
7. Murata, S., Yashiroda, H. & Tanaka, K. Molecular mechanisms of proteasome assembly. *Nat. Rev. Mol. Cell Biol.* 10, 104–15 (2009).
8. Hisamatsu, H. *et al.* Newly identified pair of proteasomal subunits regulated reciprocally by interferon gamma. *J. Exp. Med.* 183, 1807–16 (1996).
9. Seifert, U. *et al.* Immunoproteasomes preserve protein homeostasis upon interferon-induced oxidative stress. *Cell* 142, 613–24 (2010).
10. McConkey, D. J. & Zhu, K. Mechanisms of proteasome inhibitor action and resistance in cancer. *Drug Resist. Updat.* 11, 164–79 (2008).
11. Hideshima, T. *et al.* Bortezomib induces canonical nuclear factor-kappaB activation in multiple myeloma cells. *Blood* 114, 1046–52 (2009).
12. McConkey, D. J. Bortezomib paradigm shift in myeloma. *Blood* 114, 931–2 (2009).
13. Crawford, L. J., Walker, B. & Irvine, A. E. Proteasome inhibitors in cancer therapy. *J. Cell Commun. Signal.* 5, 101–10 (2011).
14. Lawrence, T. The nuclear factor NF-kappaB pathway in inflammation. *Cold Spring Harb. Perspect. Biol.* 1, a001651 (2009).
15. Qureshi, N., Morrison, D. C. & Reis, J. Proteasome protease mediated regulation of cytokine induction and inflammation. *Biochim. Biophys. Acta* 1823, 2087–93 (2012).
16. Muchamuel, T. *et al.* A selective inhibitor of the immunoproteasome subunit LMP7 blocks cytokine production and attenuates progression of experimental arthritis. *Nat. Med.* 15, 781–7 (2009).
17. Lee, S.-W., Kim, J.-H., Park, Y.-B. & Lee, S.-K. Bortezomib attenuates murine collagen-induced arthritis. *Ann. Rheum. Dis.* 68, 1761–7 (2009).
18. Pai, C.-C. S. *et al.* Treatment of chronic graft-versus-host disease with bortezomib. *Blood* 124, 1677–88 (2014).
19. Sun, K. *et al.* Inhibition of acute graft-versus-host disease with retention of graft-versus-tumor effects by the proteasome inhibitor bortezomib. *Proc. Natl. Acad. Sci. U. S. A.* 101, 8120–5 (2004).

20. Vanderlugt, C. L., Rahbe, S. M., Elliott, P. J., Dal Canto, M. C. & Miller, S. D. Treatment of established relapsing experimental autoimmune encephalomyelitis with the proteasome inhibitor PS-519. *J. Autoimmun.* 14, 205–11 (2000).
21. Adams, J. The proteasome: a suitable antineoplastic target. *Nat. Rev. Cancer* 4, 349–60 (2004).
22. Herrmann, J. *et al.* Chronic proteasome inhibition contributes to coronary atherosclerosis. *Circ. Res.* 101, 865–74 (2007).
23. Van Herck, J. L. *et al.* Proteasome inhibitor bortezomib promotes a rupture-prone plaque phenotype in ApoE-deficient mice. *Basic Res. Cardiol.* 105, 39–50 (2010).
24. Wilck, N. *et al.* Attenuation of early atherogenesis in low-density lipoprotein receptor-deficient mice by proteasome inhibition. *Arterioscler. Thromb. Vasc. Biol.* 32, 1418–26 (2012).
25. Kitamura, A. *et al.* A mutation in the immunoproteasome subunit PSMB8 causes autoinflammation and lipodystrophy in humans. *J. Clin. Invest.* 121, 4150–60 (2011).
26. Oliva, J., French, S. W., Li, J. & Bardag-Gorce, F. Proteasome inhibitor treatment reduced fatty acid, triacylglycerol and cholesterol synthesis. *Exp. Mol. Pathol.* 93, 26–34 (2012).
27. Li, N. *et al.* Relative quantification of proteasome activity by activity-based protein profiling and LC-MS/MS. *Nat. Protoc.* 8, 1155–68 (2013).
28. Li, Z. *et al.* Niacin reduces plasma CETP levels by diminishing liver macrophage content in CETP transgenic mice. *Biochem. Pharmacol.* 84, 821–9 (2012).
29. Bross, P. F. *et al.* Approval summary for bortezomib for injection in the treatment of multiple myeloma. *Clin. Cancer Res.* 10, 3954–64 (2004).
30. Reagan-Shaw, S., Nihal, M. & Ahmad, N. Dose translation from animal to human studies revisited. *FASEB J.* 22, 659–61 (2008).
31. Kalim, K. W., Basler, M., Kirk, C. J. & Groettrup, M. Immunoproteasome subunit LMP7 deficiency and inhibition suppresses Th1 and Th17 but enhances regulatory T cell differentiation. *J. Immunol.* 189, 4182–93 (2012).
32. Mehlem, A., Hagberg, C. E., Muhl, L., Eriksson, U. & Falkevall, A. Imaging of neutral lipids by oil red O for analyzing the metabolic status in health and disease. *Nat. Protoc.* 8, 1149–54 (2013).
33. Targher, G. *et al.* Relation of nonalcoholic hepatic steatosis to early carotid atherosclerosis in healthy men: role of visceral fat accumulation. *Diabetes Care* 27, 2498–500 (2004).
34. Morán-Salvador, E. *et al.* Role for PPARγ in obesity-induced hepatic steatosis as determined by hepatocyte- and macrophage-specific conditional knockouts. *FASEB J.* 25, 2538–50 (2011).
35. Semenkovich, C. F. *et al.* Lipoprotein lipase and hepatic lipase mRNA tissue specific expression, developmental regulation, and evolution. *J. Lipid Res.* 30, 423–31 (1989).
36. Hendrikx, T. *et al.* Macrophage specific caspase-1/11 deficiency protects against cholesterol crystallization and hepatic inflammation in hyperlipidemic mice. *PLoS One* 8, e78792 (2013).
37. Bieghs, V. *et al.* Trapping of oxidized LDL in lysosomes of Kupffer cells is a trigger for hepatic inflammation. *Liver Int.* 33, 1056–61 (2013).
38. Bieghs, V. *et al.* Role of scavenger receptor A and CD36 in diet-induced nonalcoholic steatohepatitis in hyperlipidemic mice. *Gastroenterology* 138, 2477–86, 2486.e1–3 (2010).
39. Babaev, V. R. *et al.* Macrophage lipoprotein lipase promotes foam cell formation and atherosclerosis in vivo. *J. Clin. Invest.* 103, 1697–705 (1999).
40. Wójcik, C. *et al.* Lovastatin and simvastatin are modulators of the proteasome. Int. J. Biochem. *Cell Biol.* 32, 957–65 (2000).
41. Rao, S. *et al.* Lovastatin-mediated G1 arrest is through inhibition of the proteasome, independent of hydroxymethyl glutaryl-CoA reductase. *Proc. Natl. Acad. Sci. U. S. A.* 96, 7797–802 (1999).
42. Otoda, T. *et al.* Proteasome dysfunction mediates obesity-induced endoplasmic reticulum stress and insulin resistance in the liver. Diabetes 62, 811–24 (2013).
43. Yavasoglu, I. et al. Cholesterol levels in patients with multiple myeloma. *Ann. Hematol.* 87, 223–8 (2008).
44. Waters, D. D. *et al.* Lipid treatment assessment project 2: a multinational survey to evaluate the proportion of patients achieving low-density lipoprotein cholesterol goals. *Circulation* 120, 28–34 (2009).
45. Superko, H. R. & King, S. Lipid management to reduce cardiovascular risk: a new strategy is required. *Circulation* 117, 560–8; discussion 568 (2008).
46. Reiner, Z. Resistance and intolerance to statins. *Nutr. Metab. Cardiovasc. Dis.* 24, 1057–66 (2014).
47. DiNicolantonio, J. J., Chatterjee, S., Lavie, C. J., Bangalore, S. & O'Keefe, J. H. Ezetimibe Plus Moderate Dose Simvastatin After Acute Coronary Syndrome: What are we IMPROVEing on? *Am. J. Med.* (2015).